JOURNAL OF
Materials
CHEMISTRY

Substitution of transition metals into azamacrocycle–gallophosphate inorganic–organic hybrid materials†

David Wragg and Russell E. Morris*

School of Chemistry, University of St. Andrews, Purdie Building, St. Andrews, UK KY16 9ST.
E-mail: rem1@st-and.ac.uk

Received 31st July 2000, Accepted 18th October 2000
First published as an Advance Article on the web 21st November 2000

Transition metals (Cu, Mn and Co) have been substituted for gallium in an azamacrocycle-containing gallium phosphate inorganic–organic hybrid material $(GaPO_4)_2(OH)F_2 \cdot Ga(C_{10}N_4H_{24})$. The substitution of the gallium by copper and manganese occurs at the octahedral site that is at the centre of the azamacrocycle complex. The effect of this substitution on the structure of the materials has been studied using Rietveld refinement against synchrotron X-ray powder diffraction data and electron spin resonance spectroscopy.

Introduction

The area of inorganic–organic hybrid materials is the focus of much current research. The combination of inorganic and organic moieties leads to both novel structural architecture and unusual properties unique to the hybrids.[1] Recently we reported the synthesis from fluoride media of cyclam–GaPO (formula $(GaPO_4)_2(OH)F_2 \cdot Ga(C_{10}N_4H_{24})$),[2] a zeolite-related gallium phosphate material containing cyclam (1,4,8,11-tetraazacyclotetradecane). This is a new type of inorganic–organic hybrid consisting of layers of a gallophosphate framework (Fig. 1) linked by a gallium–cyclam complex to form a three-dimensional structure (Fig. 1). The zeolite-related layer is composed of GaPO double four ring units (D4Rs), which have fluorine atoms occluded at their centre. Cyclam–GaPO crystallises in the orthorhombic space group *Pbcn* with $a = 13.2863$, $b = 104880$ and $c = 18.4563$ Å (room temperature). We now report further development of this structure by the substitution of transition metal ions for gallium in both the cyclam complex and the framework. The incorporation of these ions could lead to interesting magnetic and catalytic properties and prove useful in future investigations of this family of materials. In particular, the controlled substitution of functional metals into the different regions of hybrid structures of this type could lead to multifunctional materials with properties that are vastly different to those available at the present time.

The substitution of metals into gallium and aluminium phosphate materials has been widely reported, most notably the cobalt-substituted aluminophosphates (CoAPOs) developed by Thomas *et al.*[3] The substitution of several different transition metals into gallium phosphates has been reported by Chippindale and Cowley.[4] Owing to factors such as preferred coordination geometry and template-framework charge balancing it is common for the substituted materials to have novel structural architectures as in the work of Stucky *et al.*[5] and the magnesium-substituted materials STA-1 and STA-2.[6] The use of cyclam as a template in the synthesis of this type of material has also been further investigated since the initial reporting of cyclam–GaPO. Patarin and co-workers have demonstrated that a cyclam-containing GaPO can be prepared in the absence of fluorine.[7] This material has a similar structure to that of cyclam–GaPO with a gallium–cyclam complex bonded to the framework in a chain-type structure. When cyclam or a derivative of cyclam is used as a template for AlPOs the aluminium is not coordinated by the macrocycle and a different class of macrocycle-containing open framework is obtained. This, combined with the use of substitutional transition metal ions, has led to the development of STA-6 and -7 by Wright *et al.*[8] In addition to these developments using cyclam derivatives, Férey has reported MIL-1,[9] a material containing a hexaazamacrocycle as the template and the templating of zeolites X and Y by porphyrins has been reported by Khan and Hriljac.[10]

We prepared samples of cyclam–GaPO which retain their original structure with up to 20% substitution of manganese or

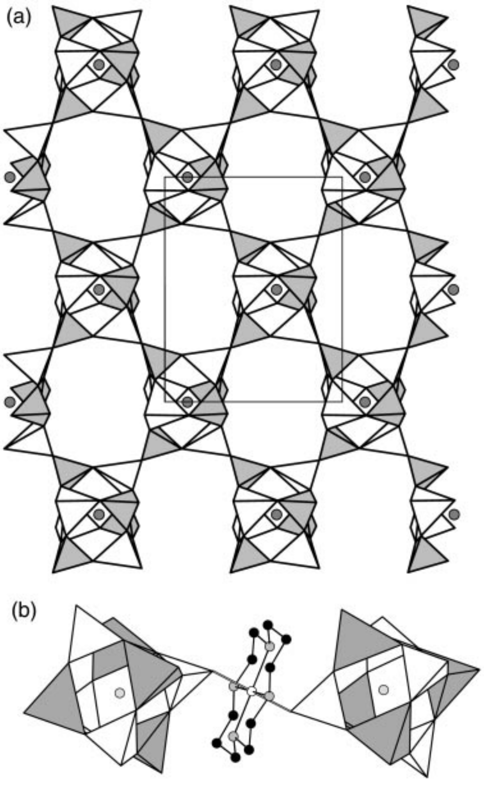

Fig. 1 The zeolite-like layer motif of cyclam–GaPO viewed in the (100) direction (a) and the linkage of the D4Rs in cyclam–GaPO by the gallium–cyclam complex (b).

---

†Electronic supplementary information (ESI) available: powder diffraction data (CCDC 1145/257). See http://www.rsc.org/suppdata/jm/b0/b006176j/

DOI: 10.1039/b006176j

Table 1 Atomic coordinates for pure gallium–cyclam–GaPO (M = Ga; from microcrystal X-ray diffraction, reference 2), and copper-substituted (20%) cyclam–GaPO (M = Cu; Rietveld refinement, this work)

	M–cyclam–GaPO (M = Ga)			M–cyclam–GaPO (M = Cu)		
	x	*y*	*z*	*x*	*y*	*z*
Ga(1)	0.8583(1)	0.2488(1)	0.7303(1)	0.8574(6)	0.2469(9)	0.7321(6)
Ga(2)	0.0337(1)	−0.0202(1)	0.6406(1)	1.0319(7)	−0.0252(8)	0.6380(4)
M(3)	0.0000	0.5000	0.5000	1.0000	0.5000	0.5000
P(4)	0.0374(1)	0.2721(1)	0.6224(1)	1.0272(18)	0.2792(18)	0.6162(10)
P(5)	0.8284(1)	−0.0443(1)	0.7243(1)	0.8302(13)	−0.0457(18)	0.7295(13)
O(1)	0.7915(2)	0.0950(3)	0.7294(2)	0.7939(20)	0.0950(23)	0.7278(26)
O(2)	0.1244(3)	−0.0865(3)	0.7044(2)	1.1218(27)	−0.0950(30)	0.7019(16)
O(3)	0.0584(3)	−0.1154(3)	0.5626(2)	1.0575(30)	−0.129(4)	0.5530(14)
O(4)	0.9271(2)	0.2866(3)	0.6470(2)	0.9221(27)	0.298(4)	0.6509(19)
O(5)	0.7593(2)	0.3694(3)	0.7060(2)	0.7602(28)	0.3682(33)	0.7033(25)
O(6)	0.0619(3)	0.1335(3)	0.6045(2)	1.0501(32)	0.1323(23)	0.6022(15)
O(7)	0.9036(3)	−0.0574(3)	0.6619(2)	0.9040(22)	−0.064(4)	0.6646(18)
O(8)	0.0529(2)	0.3529(3)	0.5560(2)	1.0765(24)	0.3371(33)	0.5479(20)
O(9)	0.8922(3)	0.3191(3)	0.8171(2)	0.8965(28)	0.308(4)	0.8187(17)
F(1)	0.0000	0.1289(4)	0.7500	1.0000	0.1289(14)	0.7500
N(1)	0.9197(3)	0.3769(4)	0.4353(2)	0.9211(30)	0.393(5)	0.4325(23)
N(2)	0.1158(3)	0.4718(4)	0.4283(2)	1.1178(28)	0.455(5)	0.4341(23)
C(1)	0.2173(3)	0.4600(5)	0.4616(3)	1.215(4)	0.466(6)	0.4576(30)
C(2)	0.9757(4)	0.3713(5)	0.3652(2)	0.969(4)	0.398(5)	0.3806(27)
C(3)	0.0872(4)	0.3604(5)	0.3822(3)	1.090(4)	0.361(6)	0.3850(32)
C(4)	0.8108(2)	0.4030(4)	0.4255(2)	0.811(4)	0.402(6)	0.4314(30)
C(5)	0.2437(2)	0.5814(4)	0.5024(2)	1.2411(34)	0.575(6)	0.5033(33)

copper for gallium, the results of cobalt substitution and the attempted substitution of nickel are also considered. The materials were characterised by powder X-ray diffraction (PXRD) and electron spin resonance (ESR) measurements.

Experimental

The substituted materials have been prepared in two ways. First by simply replacing a percentage of the gallium source ($Ga_2(SO_4)_3$, 99.9%, Aldrich) with a salt of either copper, manganese, cobalt or nickel in the normal synthesis, and secondly by replacing the cyclam with a pre-prepared and characterised metal–cyclam complex. The second method has only so far been applied to the preparation of a manganese-substituted version of cyclam GaPO.

Cyclam–GaPO was prepared by a solvothermal reaction using a mixture of pyridine (99%, Fisher) and water as the solvents. In a typical synthesis 0.2 g phosphoric acid (85% weight aqueous solution, Aldrich) was diluted with 2 ml of distilled water and 8 ml of pyridine with stirring. Gallium sulfate (0.5 g) and the metal source ($CuCl_2$, $MnCl_2$, $CoCO_3$, $NiCl_2$) were then added along with 0.25 g of cyclam (99.9%, Aldrich). 0.2 ml of HF (70% solution in pyridine) was then added and the resulting mixture aged for 30 min at room temperature with stirring to allow homogenisation of the gel. After this time the mixture was transferred to a Teflon-lined stainless steel autoclave and heated at 150 °C for 72 h. The products were recovered by vacuum filtration, washed with distilled water and acetone and dried at room temperature.

The use of a pre-reacted cyclam complex has been investigated only for manganese substitution. In this case, the 0.25 g of cyclam was replaced with the appropriate molar amount of manganese cyclam dichloride. To prepare this, $Mn(cyclam)Cl_2{\cdot}5H_2O$ was synthesised by dissolving cyclam (2.4 g, 98%, Strem) in ethanol (60 ml) and adding $MnCl_2{\cdot}4H_2O$ (0.2364 g, obtained locally). The resulting solution was stirred for 3 h, extracted into 20 ml of distilled water and acidified with 20 ml of 4 mol dm^{-3} hydrochloric acid. Green needlelike crystals were recovered (microanalysis: C, found 30.25%, calc. 28.9%; H, found 8.63%, calc. 7.3%, N, found 13.97%, calc. 13.5%) by filtration and dried at room temperature in air. The preparation of Mn–cyclam–GaPO using this complex was essentially the same as the process described above with the complex replacing cyclam and gallium sulfate (0.5 g) the only metal salt added.

EDAX analysis was carried out on the metal-substituted cyclam–GaPO samples and revealed substitution levels slightly less than expected for complete incorporation of the transition metals. For example, the 20% Mn–cyclam–GaPO sample showed substitution levels of approximately 19.1%. Examination of a number of crystallites revealed that the extra Mn was present in small amounts of a separate phase, together with a small amount of gallium rich Mn–cyclam–GaPO.

Initial identification of products was carried out by PXRD on a Phillips Xpert powder diffractometer using CuKα radiation. Further high accuracy, high resolution PXRD data were collected at room temperature on Station 2.3 of the Synchrotron Radiation Source, Daresbury, UK using an X-ray wavelength of 1.0011 Å. Samples were mounted in silica capillaries and spun at high speed on a modified Stoe spinner. ESR spectra were collected on a Bruker ES073 spectrometer at 120 K with the powder samples packed in long tipped Pasteur pipettes. The magnetic field modulation frequency was 9.53 GHz.

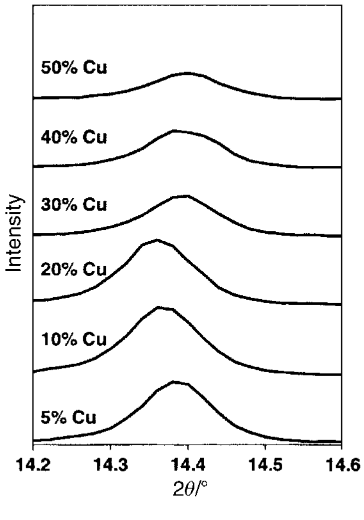

Fig. 2 The most intense peak in the PXRD pattern of Cu-substituted cyclam–GaPO. The shifting peak position is due to the structural changes when Cu replaces Ga.

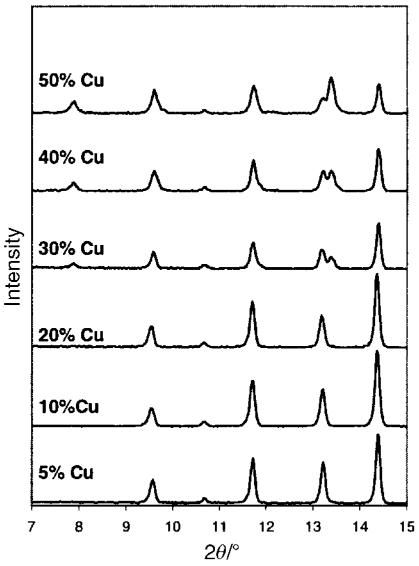

Fig. 3 PXRD patterns for samples of cyclam–GaPO containing up to 50% Cu. A secondary phase is clearly visible at 30% substitution.

Results

Full Rietveld refinement was carried out on the pure Ga–cyclam–GaPO and 20% Cu–cyclam–GaPO (Table 1) and lattice parameters were measured for all the samples. Changes in the lattice parameters are evident when comparing the PXRD profiles for Cu substitution, with the peaks clearly shifting as the level of substitution is increased (Fig. 2). Below 20% substitution the materials are pink in colour. At levels of substitution greater than 20%, however, the peak positions for the cyclam–GaPO structure return to their initial values, this corresponds with the appearance of a second phase (Fig. 3). This can be attributed to the phenomenon of phase segregation, with all the copper forming the new phase leaving pure gallophosphate cyclam–GaPO. At these levels of substitution, the products of the reactions no longer have a pink colour but a purple material is more evident. At even higher levels of substitution (40–50% Cu) the secondary phase becomes the dominant product. It is crystalline but still unidentified; it seems likely that it is some form of copper phosphate hydrate. For Mn substitution, a similar scenario is observed but with an amorphous phase becoming the dominant product at high levels of substitution.

For low levels of Cu and Mn substitution (up to 20%) the powder XRD patterns of the M-substituted cyclam–GaPO structures are similar to that of the pure gallium material. The structure was therefore not substantially altered by the substitution of these metals for gallium. As stated above Cu–cyclam–GaPO containing up to 20% copper has a pink colour, which is associated with octahedral copper(II) coordinated by nitrogen donor ligands, so it may be inferred that the first 20% of copper substituted for gallium occupies the site in the centre of the cyclam macrocycle. This is consistent with the crystal structure, which has three gallium sites. The two tetrahedral framework gallium atoms (Ga1 and Ga2) occupy general positions while the gallium (Ga3) in the cyclam complex is on a special position (0, ½, ½) with a crystallographic occupancy of 0.5. This means that 80% of the gallium atoms in the unit cell occupy the tetrahedral sites while 20% occupy sites in the gallium–cyclam complex. Using this as a model for partial occupancy of the cyclam site it was possible to carry out Rietveld refinements against synchrotron PXRD data for samples containing 5, 10 and 20% Cu substituted for Ga (¼, ½ and full occupancy of the cyclam Ga site by Cu) using the program GSAS.[11] Atomic coordinates for the pure cyclam–GaPO and 20% copper-substituted materials are given in Table 1. The fits obtained were of good quality (Fig. 4) and the refined unit cell parameters obtained show a pattern of

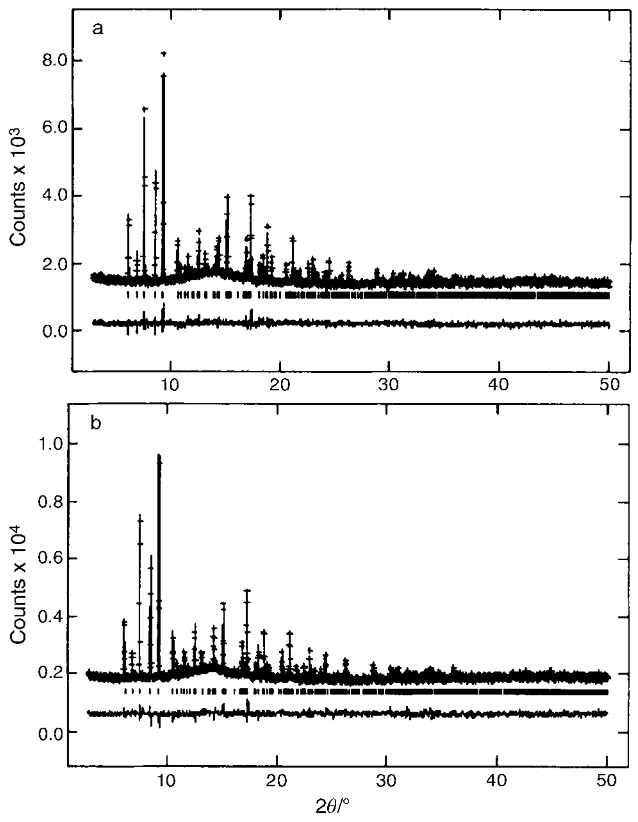

Fig. 4 Observed, calculated and difference plots for the Rietveld refinement of Ga–cyclam–GaPO (a) and 20% Cu–cyclam–GaPO (b) against synchrotron X-ray powder diffraction data.

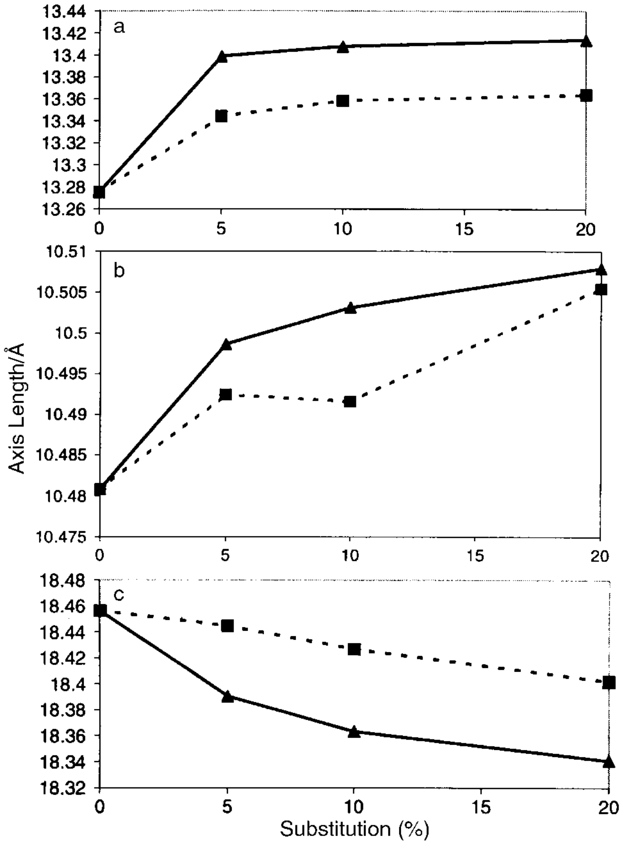

Fig. 5 The variation of lattice parameters with extent of Cu (dotted line) and Mn (solid line) substitution. The graphs show the increase in the *a*-axis (a) and *b*-axis (b), and the decrease in the *c*-axis length (c).

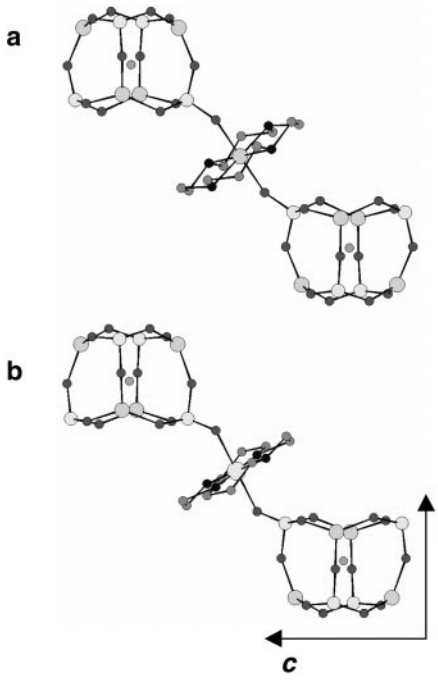

Fig. 6 Linked D4R units for cyclam–GaPO with gallium (a) and copper (b) in the complex site viewed along the crystallographic *a*-axis. The tilting of the octahedral axis of the cyclam complex is clearly illustrated.

increasing *a*- and *b*-axis length and decreasing *c*-axis length with increasing Cu substitution (Fig. 5). By applying the same model to Mn–cyclam–GaPO good Rietveld fits were obtained which gave lattice parameters showing the same trends with increasing M substitution (Fig. 5).

The lattice parameter variations are explained by changes in the substituted structures when atom positions were refined in the Rietveld process. In order to avoid refinement instability several parts of the structure were restrained to retain known conformations. The bond lengths and angles of the D4R and the cyclam ring were taken from the single crystal structure of cyclam–GaPO while the Cu–O bond lengths were taken from previously reported copper–cyclam complex structures with oxygen ligands.[12] With these restraints in place, it was possible to refine the positions of all atoms in the model without divergence. The major difference between the pure gallium- and copper-substituted structures is that the cyclam complex is pivoted about the central copper atom (Fig. 6). This causes the axial Cu–O bonds to come closer to parallel with the *a*- and *b*-axes (which therefore extend since Cu–O bonds are longer than Ga–O bonds) and moving away from the *c*-axis (the angle between O8 and the *c*-axis increases from 47.7 to 67.3°; Fig. 6). This leads to a reduction in the separation of the D4R layers from 8.034 to 7.884 Å (taking the P4–P4 distance as the measure of layer separation), and hence the contraction of the *c*-axis. The results of the full Rietveld refinement on pure gallium–cyclam–GaPO and cyclam–GaPO containing 20% Cu are presented in Tables 2 and 3. The Rietveld refinement of the pure Ga–cyclam–GaPO compared very well with the previously published microcrystal diffraction study.[2] It was not possible to fully refine the model for Mn substitution as the sample contained a small amount of an unidentified impurity. However, the results show the same trend.

For low levels of substitution (5%) in which the cyclam–GaPO structure is the only product it was possible to record the ESR spectra of both Cu- and Mn-substituted materials. Mn-substituted cyclam–GaPO shows a single peak ($g = 2.01$) with no visible hyperfine splitting, this shows that Mn is present in the sample but gives no information on its environment. A higher field instrument would be needed to provide further information. The case of Cu substitution is more informative. The pattern observed was successfully simulated (Fig. 7) using the program Simfonia[13] for Cu^{2+} (d^9, single free electron, spin 3/2). It is axially symmetric with $g_{\parallel} = 2.1823$ and $g_{\perp} = 2.05$, this suggests that the Cu is in either an axially compressed tetrahedral site or an axially strained octahedral site (tetragonal distortion).[14] Since it would be unusual to find Cu^{2+} in an axially compressed tetrahedral geometry, this lends further support to the theory that the Cu occupies only the octahedral cyclam complex site. The axial extension is explained by the Jahn–Teller effect, well documented for Cu^{2+}, similar *g* values are also observed for other d^9 ions with this site geometry (Table 3). The principal component of the hyperfine coupling is parallel to the principal axis of the site with $J = 200\ cm^{-1}$. Other components are close to zero.

When cobalt is added to the synthesis gel, the product is a pale blue material. This colour is characteristic of Co^{2+} in tetrahedral coordination, which implies that the cobalt occupies the tetrahedral sites in the gallium phosphate layers rather than the octahedral complex site. The cyclam–GaPO phase is strongly evident in the PXRD patterns at levels of substitution up to 30%; however, the intensity of the peaks rapidly decreases indicating a more amorphous character in the bulk material with cyclam–GaPO no longer the dominant product. That cobalt is incorporated into the cyclam–GaPO structure is supported by analysis of the PXRD data, which show changes in lattice parameters for Co-substituted materials and also by the strong blue colour observed in the products even at low levels of Co substitution (for which the product remains highly crystalline and exhibits no impurities). However, it is quite possible that there is a mixed substitution at both sites rather than at just one. Further work is continuing to ascertain whether this is indeed the case. At 50% substitution no cyclam–GaPO is present in the PXRD pattern of the product, only an unidentified crystalline phase. Attempts to

Table 2 Details of the Rietveld refinements of Ga–cyclam–GaPO and Cu–cyclam–GaPO (containing 20% Cu substitution for Ga)

	Ga–cyclam–GaPO	Cu–cyclam–GaPO (20% Cu)
Diffractometer	SRS station 2.3	SRS station 2.3
Wavelength/Å	1.0011	1.0011
Temperature/K	298	298
2θ range/°	3–40	3–40
Step size/°	0.1	0.1
Chemical formula	$(GaPO_4)_2(OH)F_2 \cdot Ga(C_{10}N_4H_{24})$	$(GaPO_4)_2(OH)F_2 \cdot Cu(C_{10}N_4H_{24})$
Formula weight	654.66	648.48
Space group	*Pbcn*	*Pbcn*
Unit cell dimensions/Å	$a = 13.2863(3)$	$a = 13.3645(3)$
	$b = 10.4879(2)$	$b = 10.4977(2)$
	$c = 18.4564(4)$	$c = 18.4018(5)$
Z	4	4
Number of reflections	844	812
Final *R* values	$wRp = 0.0347$ $Rp = 0.0269$	$wRp = 0.0315$ $Rp = 0.0237$
Background method	Fixed background	Fixed background

Table 3 Comparison of g values for d^9 ions in tetragonally distorted octahedral crystal fields (after reference 14) with those from Cu–cyclam–GaPO

Ion	Host	$g_{\parallel}$	$g_{\perp}$
Cu^{2+}	Cyclam–GaPO	2.183	2.050
Cu^{2+}	Copper phthalocyanine	2.165	2.045
Ag^{2+}	KCl	2.193	2.035
Au^{2+}	ZnSe	2.183	2.033

produce similar materials containing nickel have met with failure. This is probably because Ni^{2+} favours square planar coordination geometry and binds strongly to cyclam, making the cyclam–GaPO structure an unfavourable option.

Common to all of the materials described is the replacement of an ion with +3 oxidation state by one with +2. This creates an interesting situation in charge balancing with an extra negative charge to be accounted for without a significant change of structure. There are two possible mechanisms. The first and most likely is that an additional proton from the acidic reaction mixture is coordinated in the interlayer space, near to the cyclam complex or the terminal OH group attached to Ga2. The second possible explanation is that the fluorine atoms from the D4R cages of the gallophosphate layers are somehow lost. This second explanation seems highly unlikely as it is thought that the fluorine atoms play a structure-directing role in the formation of D4Rs,[15] and low M^{2+} substitution levels would require partial occupancy of the D4Rs by F^- ions. The literature on fluorinated open frameworks contains no examples of D4Rs without occluded fluorine.

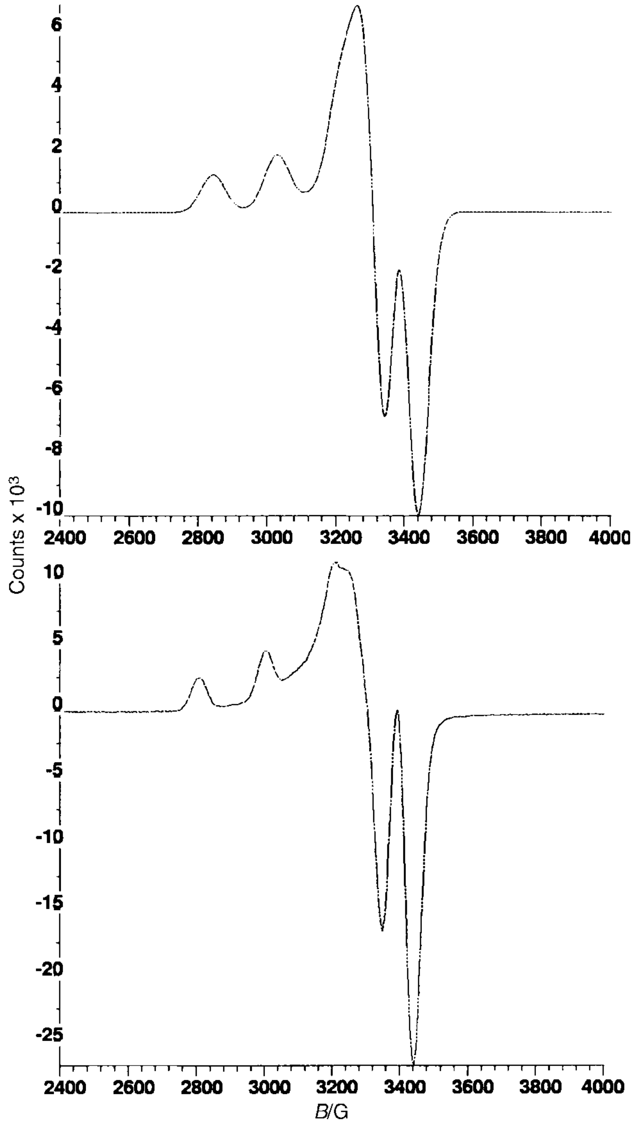

Fig. 7 Observed and simulated ESR spectra for Cu-substituted cyclam–GaPO.

Conclusions

It has been possible to prepare materials with the previously reported cyclam–GaPO structure containing transition metal ions substituted for gallium. The site in which the M^{2+} ion replaces gallium appears to depend upon the preferred coordination geometry of the ion. In the case of copper substitution, the substitutional site can be characterised from the ESR spectrum of the material. We have also provided evidence for a mechanism by which the changes in lattice parameters may be explained.

The substitutions affect the lattice parameters of the structure in a systematic manner with the *a*- and *b*-axes extending and the *c*-axis contracting for copper, cobalt and manganese substitution although the colour of the Co-substituted material suggests that the cobalt occupies a different site to the copper. Nickel cannot be substituted for gallium, as its preferred square planar geometry is not compatible with the cyclam–GaPO structure.

Acknowledgements

We thank Dr C. C. Tang for assistance in collecting the synchrotron X-ray powder diffraction data, Professors J. Walton and P. Reidi and Dr N. Poulton for assistance with the ESR measurements, Dr W. Zhou for electron microscopy and the EPSRC for financial support. R. E. M. also thanks the Royal Society for the provision of a University Research Fellowship.

References

1 D. A. Loy and K. J. Shea, *Chem. Rev.*, 1995, **95**, 1431; G. Alberti, M. Casciola, U. Costantino and R. Vivani, *Adv. Mater.*, 1996, **8**, 291.
2 D. S. Wragg, G. B. Hix and R. E. Morris, *J. Am. Chem. Soc.*, 1998, **120**, 6822.
3 P. A. Wright, R. H. Jones, S. Natarajan, R. G. Bell, J. S. Chen, M. B. Hursthouse and J. M. Thomas, *J. Chem. Soc., Chem. Commun.*, 1993, 633; P. A. Wright, S. Natarajan, J. M. Thomas, R. G. Bell, P. L. Gaiboyes, R. H. Jones and J. S. Chen, *Angew. Chem., Int. Ed. Engl.*, 1992, **31**, 1472; J. S. Chen, G. Sankar, J. M. Thomas, R. R. Xu, G. N. Greaves and D. Waller, *Chem. Mater.*, 1992, **4**, 1373.
4 A. M. Chippindale and A. R. Cowley, *Microporous Mesoporous Mater.*, 1998, **212**, 71.
5 P. Feng, X. Bu and G. D. Stucky, *Nature*, 1997, **388**, 735; X. Bu, P. Feng and G. D. Stucky, *Science*, 1997, **278**, 2080.
6 G. W. Noble, P. A. Wright, P. Lightfoot, R. E. Morris, K. J. Hudson, Å. Kvick and H. Graafsma, *Angew. Chem., Int. Ed. Engl.*, 1997, **36**, 81; G. W. Noble, P. A. Wright and Å. Kvick, *J. Chem. Soc., Dalton Trans.*, 1997, **23**, 4485.
7 P. Reinert, J. Patarin and B. Marler, *Eur. J. Solid State Inorg. Chem.*, 1998, **35**, 389.
8 P. A. Wright, M. J. Maple, A. M. Z. Slawin, V. Patinec, R. A. Aitken, S. Welsh and P. A. Cox, *J. Chem. Soc., Dalton Trans.*, 2000, 1243.
9 F. Serpaggi, T. Loiseau, F. Taulelle and G. Férey, *Microporous Mesoporous Mater.*, 1998, **20**, 197.
10 T. A. Khan and J. A. Hriljac, *Inorg. Chim. Acta*, 1999, **294**, 179.
11 R. B. Von Dreele and A. C. Larson, University of California, USA, 1995.
12 J. Emsley, M. Arif, P. A. Bates and M. B. Hursthouse, *J. Chem. Soc., Chem. Commun.*, 1988, 1387; P. A. Tasker and L. Sklar, *J. Cryst. Mol. Struct.*, 1975, **5**, 329.
13 Bruker Analytical, Karlsruhe, Germany, 1994–1996.
14 N. R. J. Poolton, J. J. Davies, J. E. Nicholls and B. J. Fitzpatrick, *J. Phys.C Solid State.*, 1987, **20**, 3553.
15 A. Matijasic, J. L. Paillaud and J. Patarin, *J. Mater. Chem.*, 2000, **10**, 1345.